ANNUAL REVIEWS

Annual Review of Chemical and Biomolecular Engineering

In Situ/Operando Characterization Techniques of Electrochemical CO_2 Reduction

Bjorn Hasa,[1,*] Yaran Zhao,[2,*] and Feng Jiao[1]

[1]Center for Catalytic Science and Technology, Department of Chemical and Biomolecular Engineering, University of Delaware, Newark, Delaware, USA; email: jiao@udel.edu

[2]BNU-HKUST Laboratory of Green Innovation, Advanced Institute of Natural Sciences, Beijing Normal University, Zhuhai, China

Annu. Rev. Chem. Biomol. Eng. 2023. 14:165–85

First published as a Review in Advance on March 8, 2023

The *Annual Review of Chemical and Biomolecular Engineering* is online at chembioeng.annualreviews.org

https://doi.org/10.1146/annurev-chembioeng-101121-071735

*These authors contributed equally to this article

Keywords

carbon dioxide electroreduction, advanced characterization techniques, mechanistic insights, catalyst, electrolyte, reaction intermediates

Abstract

Electrocatalytic conversion of carbon dioxide to valuable chemicals and fuels driven by renewable energy plays a crucial role in achieving net-zero carbon emissions. Understanding the structure–activity relationship and the reaction mechanism is significant for tuning electrocatalyst selectivity. Therefore, characterizing catalyst dynamic evolution and reaction intermediates under reaction conditions is necessary but still challenging. We first summarize the most recent progress in mechanistic understanding of heterogeneous CO_2/CO reduction using in situ/operando techniques, including surface-enhanced vibrational spectroscopies, X-ray- and electron-based techniques, and mass spectroscopy, along with discussing remaining limitations. We then offer insights and perspectives to accelerate the future development of in situ/operando techniques.

INTRODUCTION

CO_2 concentrations in the atmosphere are rising primarily due to fossil fuel use for energy production. According to the 2019 State of the Climate, the atmospheric CO_2 global growth rate was approximately 2.5 ± 0.1 parts per million (ppm) in 2019, four times higher than in the 1960s (0.6 ± 0.1 ppm). Given CO_2 emissions' detrimental impact on climate change, there is a need to effectively reduce the observed increasing rate. Comprehensive efforts to address CO_2 emissions include its capture and use as an abundant building block for producing chemicals and fuels (1). Among the CO_2 conversion technologies, electrochemical CO_2 reduction reaction (eCO_2RR) has attracted widespread technical and scientific attention to close the carbon cycle. In particular, by using green electrons produced via low-cost and clean renewable sources as an energy input, CO_2 and water can be converted into chemical compounds (2–5). This process also provides an attractive way to tackle the intermittent issues associated with the nature of renewable energy sources by storing excess electrical energy into chemical bonds.

Significant and continuous progress has been observed in the field of CO_2 electroreduction over the last decade. However, understanding the reaction mechanism remains challenging due to the process complexity, which derives from proton/electron transfer and numerous highly reactive intermediates. Probing the relationship between the catalyst structure, product selectivity, and reaction intermediates during electrochemical processes will provide knowledge fundamental to designing better catalysts, reactors, and interfaces. Ex situ techniques (diffraction, microscopic, and spectroscopic) can provide helpful information about the electrode's structural, compositional, chemical, and physical properties. However, use of only ex situ techniques may not be sufficient to understand mechanistic details under realistic conditions given the dynamic nature of the triple-phase region (electrolyte–catalyst–reactant). In situ/operando measurements can provide valuable information regarding the catalyst surface, electrode–electrolyte interface, and product and reaction intermediates (6–10). The term in situ means to analyze the material under conditions similar to those in electrochemical operation, which provides better mechanistic insights but is hampered by the specific electrochemical setup. The term operando indicates testing an electrochemical device with a catalyst of interest in a realistic application environment (such as holding at a higher current) (11).

In situ/operando techniques can shed light on different issues during the CO_2 electrochemical reduction (12–14), such as (*a*) surface morphology, reconstruction, state, and stability; (*b*) determination of active sites; (*c*) the electrode–electrolyte interface; and (*d*) identification of reaction intermediates and products. As summarized in **Figure 1**, widely used in situ/operando techniques include surface-enhanced Raman spectroscopy (SERS) (15, 16), surface-enhanced infrared absorption spectroscopy (SEIRAS) (17, 18), mass spectrometry (MS) (19), X-ray absorption spectroscopy (XAS) (20, 21), X-ray diffraction (XRD) (22), transmission electron microscopy (TEM) (23), and atomic force microscopy (AFM) (24).

We highlight the evolution of the catalyst and the reaction intermediates/products during eCO_2RR/eCORR by using in situ/operando characterizations. We first discuss the operating principles and knowledge that can be gained from each technique. We then use case studies to illustrate the ability of these advanced characterizations to provide essential information during the electrolysis process, along with discussing each method's limitations. Finally, we provide concluding remarks and perspectives on how these advanced characterization techniques can be applied and integrated further to elucidate the phenomena that govern eCO_2RR activity and selectivity.

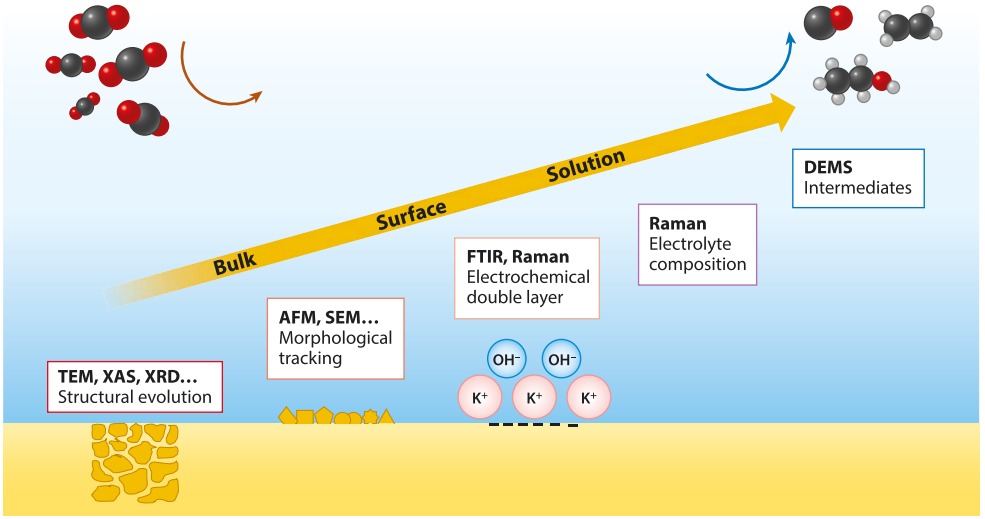

Figure 1

Overview of in situ/operando techniques used in CO_2 electroreduction. Transmission electron microscopy (TEM), X-ray absorption spectroscopy (XAS), and X-ray diffraction (XRD) provide information for the bulk catalyst. Atomic force microscopy (AFM) and scanning electron microscopy (SEM) contribute to surface analysis. Fourier transform infrared (FTIR) and Raman spectroscopy highlight the catalyst–electrolyte interface. Differential electrochemical mass spectrometry (DEMS) detects reaction intermediates and products.

SURFACE STRUCTURE EVOLUTION

Atomic Force Microscopy

In situ/operando AFM is a typical force-based method that provides topographical images through the probe's interaction with the surface and can visualize the surface evolution with high resolution (100 μm to less than 1 μm), enabling more in-depth insights into electrochemical reaction mechanisms. An AFM consists of a laser, a photodetector, and a small tip supported in a cantilever. The tip is made of silicon or silicon nitride and approaches the sample in interatomic distances (approximately 10 Å). It is 3–15 μm in length and is located at the edge of the cantilever (100–500 μm in length). The tip's interaction with the electrode due to attractive or repulsive forces causes negative or positive bending of the cantilever. This displacement of the tip as it scans the electrode surface is monitored through a laser beam reflected off the cantilever. A photosensitive detector analyzes the reflected laser beam by tracking the motion of the probe. Detector sensitivity must be calibrated to correlate the measured voltage with the moving distance.

To date, research studies with in situ AFM have examined catalyst morphology in a simple batch reactor (from polyether ether ketone) containing three electrodes (**Figure 2*a***). This experimental setup requires dissolved CO_2 as a feedstock, limiting its application for low–current density studies. However, the AFM configuration has several advantages over electron microscope techniques (see below), primarily its versatility in taking measurements in air or aqueous environments rather than in a high vacuum.

AFM analysis revealed that sample immersion in the electrolyte leads to immediate surface reconstruction. The applied potential affects the well-defined catalyst structure, which undergoes complete reformation in terms of particle shape, size, and surface roughness (**Figure 3*a***).

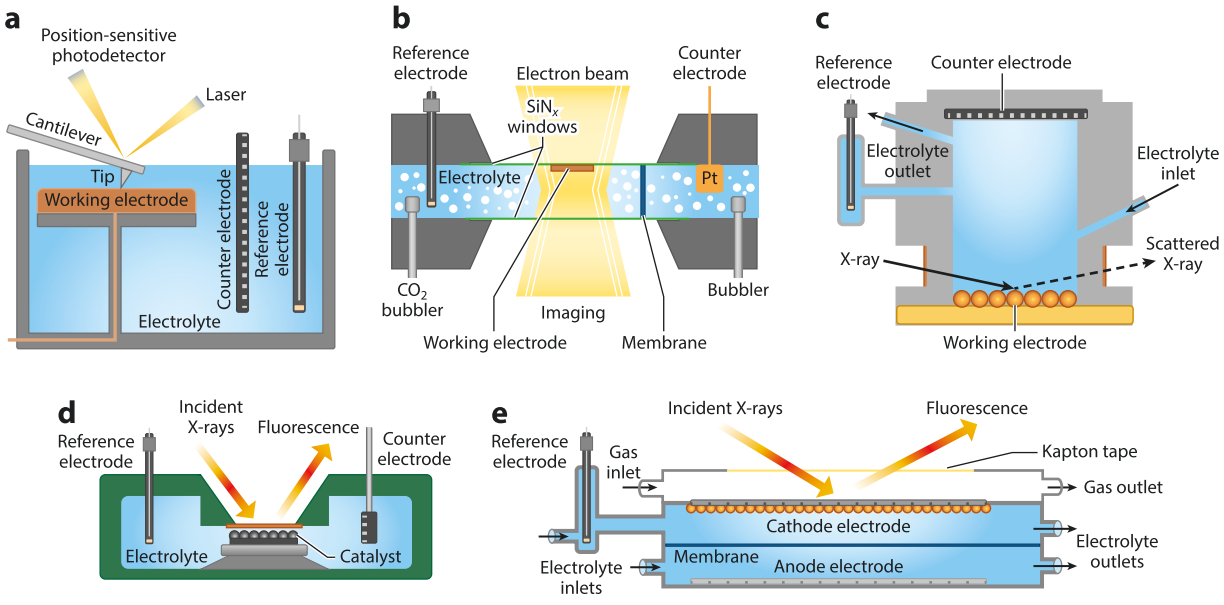

Figure 2

Various in situ/operando electrochemical cell designs used for catalyst characterization. (*a*) Batch cell for atomic force microscopy. (*b*) Gas and liquid leakage-free cell for in situ scanning transmission electron microscopy. (*c*) Schematic of the cell with a flow electrolyte system used for in situ X-ray diffraction investigations. (*d*) Batch and (*e*) flow electrochemical cells used for in situ/operando X-ray absorption spectroscopy analysis.

Operando experiments demonstrated that well-defined Cu (200-nm cube size) changed completely during CO_2 electrolysis (25). Grosse et al. (25) observed surface reconstruction, shape changes, and shorter edge length right after starting CO_2 electrolysis at a constant potential of −1.1 V versus RHE (reversible hydrogen electrode). They observed an additional 10% loss in particle size and shape reforming (spherical) after 3 h of electrolysis at −1.1 V versus RHE. In contrast, the larger cube sizes (e.g., 320 and 580 nm) had higher resistance to morphological changes, resulting in remarkable performance during CO_2 reduction. In another study, Jiang et al. (26) highlighted the trade-off between surface roughness and the fraction of Cu(100). The increased roughening of the surface led to a high fraction of Cu(100) facets, resulting in improved selectivity for multicarbon products, especially oxygenates such as ethanol and n-propanol. However, a highly roughened surface favors dimer or trimer formation, enhancing the CH_4 production rate. This work demonstrates the importance of the surface topography for product selectivity during CO_2 electroreduction.

These studies highlight the fact that AFM has impacted research across CO_2 reduction, revealing and visualizing the relationship between interfacial, morphological, and electrochemical properties. Although operando AFM can provide useful information regarding surface evolution, several remaining challenges prevent this advanced method's widespread use in the CO_2 electroreduction field. For example, AFM may fail to visualize surface evolution at high reaction rates due to low-speed imaging. In addition, AFM cannot provide insights about chemical transformation, limiting the scope of interpretation to material evolution. Last, tip–sample interactions should also be considered when analyzing data from AFM, because AFM analysis requires the probe to be close to the electrode surface, affecting the electronic field close to the surface.

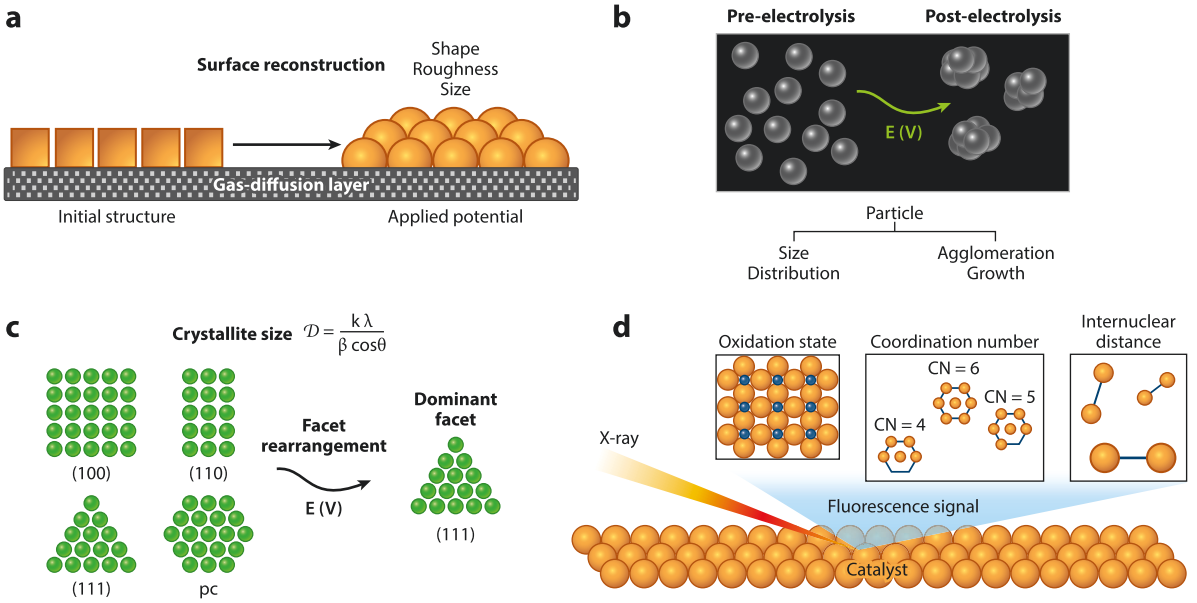

Figure 3

In situ/operando techniques used for catalyst characterization. (*a*) Atomic force microscopy showing catalyst reconstruction under operation conditions. (*b*) Scanning transmission electron microscopy visualizes particle agglomeration and growth process. (*c*) X-ray diffraction defines catalyst facets and measures crystallite size changes under electrolysis. (*d*) X-ray adsorption spectroscopy analysis is a bulk technique that provides information about the chemical state, coordination number, and interatomic distance.

Scanning Transmission Electron Microscopy

Both scanning transmission electron microscopy (STEM) and AFM are used to characterize electrocatalyst morphological and compositional features at atomic resolution (27, 28). (S)TEM involves use of electrons to generate magnified images. A high–electron energy beam (e.g., 60–350 eV) is transmitted through a specimen to project an image onto a fluorescent screen. Optional objective apertures can affect the contrast by blocking high-angle diffracted electrons. The image passes the column through the intermediate and projector lenses, where it is enlarged. The enlarged image strikes the phosphor screen, generating light and allowing the user to observe the image. Because TEM is a transmission method, the darker areas depict the area through which fewer electrons are transmitted. In contrast, the lighter areas of the image represent those areas of the sample that feature more electron transmission.

Designing a liquid TEM cell is challenging because it should be integrated into a TEM holder consisting of two microelectromechanically based chips, an electrochemical and a spacer chip, separated by another spacer chip (500 nm) (**Figure 2*b***). To maintain the chamber at ultrahigh vacuum, the electrochemical cell should have an electron-transparent and high–flexural strength window. The SiN_x windows are thin and robust, preventing the liquid electrolyte from entering into the vacuum chamber and allowing electron beam penetration. To date, the SiN_x windows (~50 nm) have been widely used for in situ/operando (S)TEM measurements. The thin windows allow electron scattering, enabling direct visualization of structural and chemical changes in the sample. In general, the reference and counter electrodes are placed outside the electron transparent area. This in situ configuration can achieve a resolution of 30 images per second in 5-nm spatial resolution (29).

Understanding catalyst modification under steady-state and transient operations is crucial when examining surface reconstruction. This is particularly important considering the high surface energy and mobility of Cu nanoparticles, which subsequently lead to particle agglomeration and growth, impacting CO_2 reduction performance (**Figure 3*b***). Vavra et al. (30) studied the transformation of spherical Cu nanoparticles during CO_2RR. Initially, spherical Cu nanoparticles are not selective toward a single product; however, they favor C–C coupling after surface transformation. The authors used TEM to perform in situ tracking of nanoparticle evolution induced by cathodic bias. Combining XAS and TEM analysis, they attributed the particle size increase to the reduction of aqueous Cu ions generated by the chemical dissolution of the Cu_2O phase or during the electrochemical reduction of Cu_2O to Cu. Small particles show a higher tendency to dissolve, harming electrolysis performance. On the other hand, larger nanoparticles display higher resistance to surface modification, most likely due to their high surface-to-volume ratio. Thus, surface reconstruction under reaction conditions depends on the initial particle size and can affect catalyst selectivity and stability.

Vavra et al.'s (30) study emphasizes the advantages of in situ (S)TEM to visualize the catalyst's real-time dynamic evolution. However, more work is required to define the relationship between the nanoscale catalyst changes and product selectivity. The operando analysis requires high electron-beam intensity to pass through the SiN_x window (20–50 nm), the electrolyte layer, and the bubbles produced. The high-intensity electron beam can permanently damage and polarize the catalyst surface and induce atom mobility. Therefore, deconvoluting the beam's contribution to surface reconstruction is challenging.

X-Ray Diffraction

XRD is an analytical technique that can determine a sample's crystallographic structure. It works based on a monochromatic X-ray beam's elastic scattering at specific angles from each lattice plane set (31). Briefly, the interaction of the incident X-ray beam with the electrons of the sample produces a diffracted X-ray beam satisfying Bragg's law ($n\lambda = 2d \sin\theta$). This scattered X-ray can be measured as a function of the sample orientation and the detector. The detector analyzes all possible lattice diffraction directions when the samples are scanned through the angle range of 2θ. Generally, in situ XRD reveals chemical composition information such as the evolution of crystal structure, phase, and orientation, as well as other structural parameters, such as average crystallite size, crystal defects, and lattice parameters. The real-time XRD spectra contribute to identifying active sites and their phase transformation and degradation. Data acquisition rates with a short time resolution are achievable.

The in situ XRD cell requires the existence of a transparent window, as shown in **Figure 2*c***. The electrolyte choice, X-ray source, and collection mode (such as reflection or transmission) should be considered carefully. The materials should be suitable for electrolyte-based experiments. Concerning data collection, reflection geometry is used mainly on laboratory diffractometers (two windows are required), in contrast to transmission geometry for synchrotron sources. Finally, the cell configuration must be designed carefully for the sample holders of the X-ray machines that will host it, challenging the design of an ideal in situ XRD cell.

XRD can track the evolution of crystal structure, composition, and crystallite particle size, thus providing information about the active sites and their degradation under reducing bias. Earlier reports examined changes in catalyst surface composition and morphology under CO_2/CO reduction conditions. Operando grazing incidence X-ray diffraction experiments on polycrystalline Cu showed that the $Cu_2O(111)$ was entirely reduced to the metallic Cu(111) at cathodic potentials (32) (**Figure 3*c***). Another study employed operando XRD and studied the impact of various additives on product selectivity using polycrystalline Cu (33). The intensity of the oxide phases

[Cu_2O(110) and Cu2O(111)] decays independently of the used additives. Similar behavior is also observed for the structural transition of Cu_2O(220) to Cu(200) (10). The authors also showed that the mean crystallite size calculated by the Scherrer equation drops from 13.3 nm to 6.7 nm at potentials below −0.2 V versus RHE. These studies explain why the initial oxidation state, or the polycrystalline Cu precursor structure, does not significantly affect the CO_2/CO reduction activity.

Lattice parameter evolution during electrolysis may lead to a better understanding of how and why surface restructuring changes catalyst activity and selectivity during CO_2RR (34). For example, in situ XRD spectra show Pd phase transformation into β-phase palladium hydride (PdH) (35). The authors observed 3.3% lattice expansion at a potential lower than −0.2 V versus RHE, which was attributed to the formation of β-phase PdH. The formation of the beta-phase lowers the binding energy of both adsorbed CO* and H*, tuning the catalyst selectivity toward producing CO and H_2.

In situ/operando XRD is a bulk technique capable of analyzing catalysts with well-defined crystalline structures. Achieving an informative signal for low-crystallinity or amorphous samples and molecular catalysts is challenging. Computer modeling and simulations should be used to interpret the obtained data to understand the diffraction of amorphous materials. Also, faster acquisition rates would be highly beneficial to study materials transformation at high reaction rates.

X-Ray Absorption Spectroscopy

XAS uses synchrotron radiation to probe the chemical or structural information of a catalyst. The XAS spectrum can be separated into two regions based on XAS features before and after the edge, known as X-ray absorption near-edge structure (XANES), and the remaining spectrum, which is extended to a few thousand electronvolts, called extended X-ray absorption fine structure (EXAFS). The observed XANES features arise from electrons' transition from occupied to unoccupied states, highlighting information about catalyst oxidation state and electronic structure. In general, the interpretation of XANES provides qualitative analysis; however, semiquantitative analysis can be obtained using linear combination analysis. After the edge, the EXAFS signal oscillations' origin derives from the ejected photoelectron interaction of the adsorbing atom with the electrostatic field of neighboring atoms. EXAFS is sensitive to the coordination environment, making it a powerful tool for quantitatively determining coordination number, bond length, and disorder factor. A recent review on in situ/operando XAS discusses this method's operating principles, challenges, and detection modes (36).

The last decade has been marked by drastic developments in in situ and operando characterization XAS techniques, making it probably the most widely used advanced technique in the CO_2 electroreduction field. This advanced technique requires a relatively simple cell design made with polyether ether ketone, which is electrically insulated and chemically inert. Many different cell designs (batch or flow reactors) have been proposed and are optimized for various applications during CO_2 reduction (**Figure 2*d*,*e***). Operando XAS studies use catalysts deposited on conducting carbon-based electrodes due to the negligible background from the carbon support, especially within the hard X-ray regime. This is the most significant advantage of the XAS method compared to other spectroscopic techniques. Despite the cell's simple design, some requirements remain when using these configurations in in situ and operando analysis. First, the working electrode must simultaneously ensure a uniform current density and potential distribution. In addition, the ohmic drop between the reference and working electrode should be minimal. Second, the window must be transparent to X-rays and, simultaneously, impermeable and corrosion resistant. Third, the X-ray's optical path should be minimized to avoid its absorption by the electrolyte. A thick electrolyte layer could lead to signal scattering and attenuation, hindering XAS data

acquisition. Fourth, bubble management should be considered carefully, especially in a batch reactor, to maximize the signal-to-noise ratio.

CO_2RR activity and selectivity are directly related to catalyst properties (e.g., oxidation state, catalyst structure, bond length, coordination numbers) (**Figure 3*d***). Thus, in situ and operando XAS analysis is indispensable to elucidate the nature of the active sites and understand how catalyst transformation is correlated with kinetics and product selectivity.

To elucidate the impact of CuZn alloy oxidation state and structure on CO_2RR selectivity, Jeon et al. (37) performed XAFS measurements under operando conditions. Selected Cu and Zn K-edge XANES spectra of $Cu_{50}Zn_{50}$ during CO_2RR showed that the Cu and Zn oxidation states were +2. Both Cu and Zn are reduced under negative bias, showing a similar spectrum with Cu and Zn foils. The time-dependent data revealed that modifying Cu with ZnO tunes the CO_2RR selectivity toward methane at the beginning of the reaction. The reduction of ZnO to metallic Zn and its enhanced interaction with Cu led to the exclusive production of CO and H_2. These useful insights show how the catalyst's chemical state changes and the interaction of active sites can tune CO_2RR selectivity.

The EXAFS spectrum can provide a detailed quantitative analysis of local structure and dynamics because it is more sensitive to the environment's geometry around the neighboring atoms. Studies have shown that the local catalyst environment evolves during electrolysis, changing the coordination number and interatomic bond length (3, 38–42). For example, Moller et al. (20) observed significant time-dependent evolution in the metallic Cu–Cu bond accompanied by a decrease in the Cu_2O-related peaks. Quantitative analysis of EXAFS data demonstrated that the interatomic distances of Cu–Cu and Cu–O are independent of the reaction time or applied potential. On the other hand, the coordination numbers of Cu–Cu and Cu–O increased and decreased, respectively. The Cu–Cu coordination number was remarkably smaller than the anticipated theoretical value, indicating the existence of undercoordinated Cu sites. Undercoordinated sites promote binding of CO and oxide-derived Cu, resulting in enhanced electrocatalytic activity (43).

In the aforementioned studies, the XAS investigations were performed in a batch-type electrochemical cell, where mass transfer limitations arise due to the low solubility of CO_2/CO in aqueous electrolytes. Because the catalyst's chemical state and the local environment are sensitive to the reaction rate, the nature of the catalyst must be monitored under high practical current densities. For example, a recent report conducted in a gas-fed device revealed no correlation between Cu oxidation state and catalyst performance, ruling out the role of Cu_2O or CuO in the enhanced activity and selectivity toward C_2H_4 (44). This critical finding emphasizes the importance of operando analysis at high reaction rates, where the role of the oxidized species in CO_2RR performance remains unclear.

Operando XAS measurements are crucial to understanding electrochemical processes such as CO_2/CO reduction because of the insights regarding the electronic and geometric structure of the catalyst. XAS experimental analysis should be designed carefully given this method's inability to identify atom coordination numbers with similar masses.

SURFACE SPECIES AND INTERMEDIATES

Raman Spectroscopy

Raman spectroscopy collects the light that scatters after the laser reacts with the molecules, which provides characteristic vibrations that are used extensively to determine and identify molecular structures. SERS enables the detection of molecules with weak scattering cross-sections on roughed Cu, Ag, and Au surfaces via a localized surface plasmon resonance effect (45). The enhancement can also be realized on planar electrodes with shell-isolated nanoparticles (SHINs,

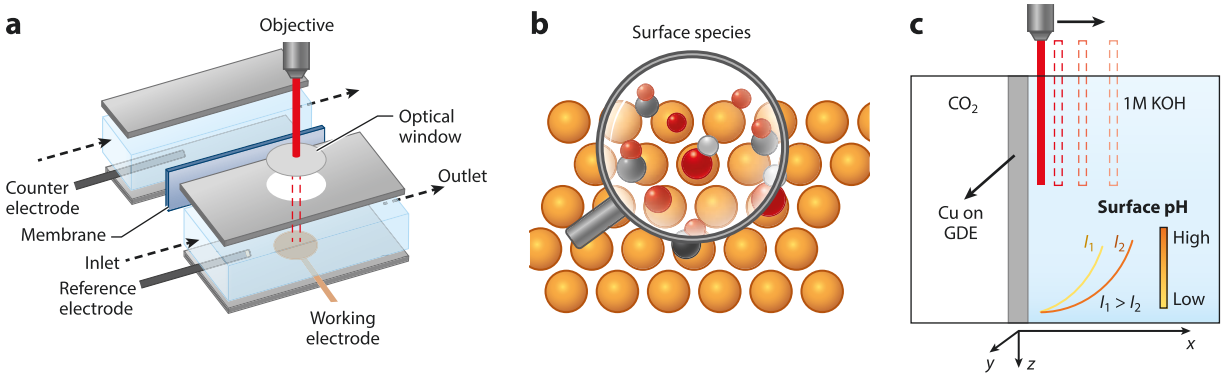

Figure 4

(*a*) Schematic of the electrochemical Raman cell design. (*b*) In situ surface-enhanced Raman spectroscopy monitoring of the surface species and intermediates on metal catalyst surface. (*c*) The determination of surface pH near the gas-diffusion electrode (GDE) surface by Raman spectroscopy.

silica-encapsulated gold nanoparticles) (46). SERS has high surface sensitivity/selectivity and is powerful in tracking the formation and transformation of surface species. At the same time, the weak scattering of H_2O molecules simplifies in situ measurement in an aqueous electrolyte. In an electrochemical Raman cell (**Figure 4*a***), two compartments are separated by an ion-exchange membrane. Cu nanoparticles deposited on a Cu foil or gas-diffusion electrode act as working electrodes. The CO- or CO_2-saturated electrolyte flows through the working electrode channel to immediately remove the hydrogen bubbles generating under negative potentials. A similar configuration has been used to detect the transformation of metal oxide or oxide-derived alloy catalysts (47, 48) and the evolution of reaction intermediates (49). In this section, we focus on the in situ SERS detection of species on Cu and local pH determination in alkaline environments.

Cu is the most efficient metal catalyst to convert CO_2 or CO to valuable oxygenates and hydrocarbons. Understanding the surface species and intermediates on Cu under reaction conditions is critical for future catalyst design and engineering. We employed SERS and investigated the surface species on five different Cu catalysts, including Cu foil, Cu nanoparticles, Cu microparticles, electrochemically deposited Cu, and oxide-derived Cu (15) (**Figure 4*c***). SHINs are added onto the Cu foil surface to enhance the Raman signal. The existence of multiple Cu oxide and hydroxide, i.e., CuO_x and $CuO_x/(OH)_y$, is identified on all surfaces under potentials as negative as −0.8 V versus RHE. The relative abundance on Cu foil compared with other catalysts is attributed to the initial oxidative state of the surface before applying reductive potential, which is confirmed by using a square wave potential switching between a positive potential and −0.4 V versus RHE. Interestingly, the surface oxide species are dependent on the electrolyte's pH. $CuO_x/(OH)_y$ species are absent in near-neutral electrolyte 0.1 M $KHCO_3$ (pH = 8.9), and its potential onset shifts to be more positive as electrolyte alkalinity increases (16). However, these oxygen-containing species' decisive role in CORR selectivity and reactivity remains ambiguous. Recently, the surface hydroxyl species, which is generated due to the introduction of a low concentration of O_2, was found to dramatically enhance eCO_2RR reactivity and selectivity (50). Note that SERS is a semiquantitative method because the enhancement factor depends strongly on enhanced electric field strength and distance. Because the absolute quantification of surface species is impossible, we usually assume the Raman cross-sections are the same for all species.

CO is an important surface species during CO_2RR or CORR, and its adsorption is usually used to assess the electronic structure of the metal catalysts or catalyst–electrolyte interactions (40, 51).

For example, the shift from linearly to bridge-bonded CO at high pH is attributed to the increased interaction between the Cu surface and cations (52). Anions could also cause catalyst restructuring (16). As C≡O stretching has a stronger infrared (IR) absorption than Raman scattering, more molecular-level insights from CO adsorption would be discussed in the IR spectroscopy section. SERS has advantages in identifying the bonds in a low frequency between 50 and 1,000 cm^{-1}. For example, the metal–carbon vibrations between the metal surface and CO are determined (Cu–C, 365 cm^{-1}; Ag–C, 490 cm^{-1}) (53). Unfortunately, the low concentration limits their detection and assignment. To overcome this challenge, a flow cell can be employed to achieve high reaction rates and accumulation of surface species (54). Applying a long-working-distance water-immersion objective to get rid of the interference from the liquid is also an attractive alternative (55, 56).

Determining local electrode pH is another important application of Raman spectroscopy in CO_2RR. The pH distribution near the electrode surface is critical for understanding how surface pH impacts reactivity and selectivity. Lu et al. (57) used a specially designed Raman flow cell with the laser beam vertical to the electrode surface, enabling determination of the pH gradient near the electrode surface (40–120 μm) in an alkaline solution (**Figure 4*b***). Based on the concentration of HCO_3^- and CO_3^{2-}, the pH distribution dependent on current densities is illustrated, showing that the reaction between CO_2 and KOH leads to a noticeable pH decrease (57). Interestingly, the local pH at the electrolyte–electrode interface decreases under potentials where initial surface oxide reduction but no CO_2RR takes place. The detection of malachite [$Cu_2(OH)_2CO_3$] on the surface may be responsible for this pH decrease (58). This precipitation persists under CO_2RR conditions, consistent with our previous observation that Cu oxygen species are present on CuO-rich surfaces at very negative potentials (15). The spectroscopically detected pH values in a flow cell are highly consistent with the calculated results if pH values at $x = 100$ μm are considered (59). However, the limitation of detection for the pH value is less than 13 because the relatively low pK_a value (10.3) for HCO_3^- significantly limits the accurate pH determination at higher reaction rates and in a more alkaline electrolyte. Developing appropriate pH descriptors and pH sensors with high pK_a values could be a possible way to address this issue, as with, for example, phosphate ions (HPO_4^-, p$K_a = 12.6$) in a recent IR study (60).

SERS can also be employed to exploit a molecular catalyst's catalytic mechanism. For example, Wright et al. (61) recently proposed a possible CO_2RR mechanism on nickel bis(terpyridine) complex by confining the molecules into a gap composed of Au planar and nanoparticles, where the strong plasmatic effect greatly enhances the signal. However, the complex peak assignment limits spectroscopic identification because the standards for most intermediates are unavailable. Density functional theory (DFT) calculations and isotope labeling are helpful in this regard.

Surface-Enhanced Infrared Absorption Spectroscopy

SEIRAS with the attenuated total reflection (ATR) mode is one of the most popular techniques in spectroelectrochemistry. Similar to the Raman cell, the SEIRAS cell contains two compartments that are separated by a piece of Nafion membrane (**Figure 5*a***). A thin metal catalyst layer is deposited onto a Si (or Ge) crystal, which acts as the working electrode. The IR beam internally reflects off the Si–metal interface, generating an evanescent wave that penetrates into the solution (**Figure 5*b***). The metal layer enhances the evanescent wave, allowing detection of only the species near the electrode (1–10 nm). This high surface sensitivity enables SEIRAS to in situ identify surface species and reaction intermediates generated during CO_2RR/CORR.

CO is the most common intermediate during eCO_2RR, and the strong IR light absorption makes CO species ideal probe molecules in SEIRAS tests. Because CO adsorbs within the inner Helmholtz layer (**Figure 5*b***), its vibration is extremely sensitive to local microenvironments,

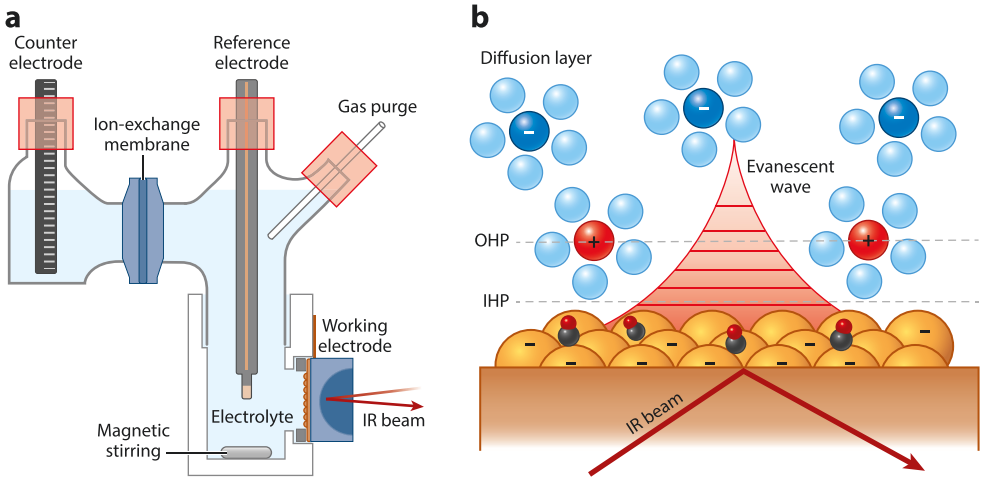

Figure 5

(*a*) Schematic of electrochemical ATR-SEIRAS cell design. (*b*) Schematic of the electrochemical double layer in SEIRAS experiments. Abbreviations: ATR, attenuated total reflection; IHP, inner Helmholtz plane; IR, infrared; OHP, outer Helmholtz plane; SEIRAS, surface-enhanced infrared absorption spectroscopy.

including surface coverage, applied potential, metal surface structure, metal oxidation state (41), electrolyte cations/anions, and mass transportation (62). SEIRAS is sensitive enough to detect CO adsorption variation, including peak configuration, Stark tuning shift, and peak intensity, upon small disturbances from local microenvironments. For example, the reversible reconstruction of Cu catalyst during eCO_2RR has been detected by the reversible appearance and disappearance of a new CO adsorption peak at low frequency (63). Of note, C≡O stretching frequency of atop-bound CO is not straightforward to distinguish between two ubiquitous surface facets, Cu(111) and Cu(100), due to the saturation coverage of CO (64). By limiting the CO coverage, different predominant surface facets on two types of Cu films could be distinguished based on CO adsorption energy on terrace and defect sites. The preference adsorption of CO on a Cu(100) surface has also been demonstrated to be more favorable to C_2H_4 production, which is in agreement with the observation of that on oxide-derived Cu with SEIRAS (65). Careful analysis should be conducted when comparing the results from Cu films used in SEIRAS with that on polycrystalline Cu catalysts during CO_2RR. Additionally, the surface concentration change of CO has been used to elucidate the mechanism of plasmon-enhanced CO_2 conversion on Ag under light illumination. The desorption of CO from the surface is accelerated in the light due to the transfer of excited electrons generated through localized surface plasmon resonance relaxation on the Ag surface to the occupied molecular orbitals of CO (66).

Because directly probing the electrochemical interface remains challenging, CO molecules have been used in SEIRAS to investigate the effect of the electrolyte components on CO_2RR reactivity. For example, because changes in the interfacial electric field can cause shifts in vibrational bands, Stark tuning of linearly bonded CO has been used to estimate the electric field for four organic cations in CORR (67). Recently, increased stark tuning has been observed as the size of hydrated alkali metal cations decreases from Li^+ to K^+ in the double layer, which indicates an enhanced electric field strength that is likely responsible for the improved C_{2+} product selectivity (17). However, related factors other than the electric field, such as the interaction with interfacial water (67) and the nonelectric field (17), also must be considered to determine CORR reactivity and selectivity.

Beyond CO, SEIRAS plays a critical role in determining the reaction intermediates and distinguishing reaction pathways during eCO_2RR. For example, the carboxyl intermediate *COOH has been proved on an Ag electrode, which is highly selective for CO production, indicating the first step of proton-coupled electron transfer (68). This step is potential dependent because $*COO^-$ also is detected under lower potentials, suggesting the coexistence of proton-coupled electron transfer and sequential electron and proton transfer processes. The intermediates in C1 (CH_4) and C2 (C_2H_4) pathways are also determined respectively on two selective Cu catalysts (69). *CHO is the intermediate for the CH_4 production pathway, whereas dimer *OCCO is the intermediate in the C–C coupling process for C_2H_4. The dimerization pathway is isolated from the C1 pathway. The fast dimerization kinetics of *CO under high frequency observed on time-resolved ATR-SEIRAS suggest these CO-binding sites are likely the active sites for fast C–C coupling. The hydrogenated dimer intermediate *OCCOH is also observed on the Cu(100) surface, which has been demonstrated to be the origin of C_2H_4 products (70).

Although ATR-SEIRAS has been employed successfully to determine the intermediates during CO_2RR/CORR, the conclusive active sites on Cu are still inconsistent because several possible active sites have been involved, such as oxidative state (41, 71, 72), grain boundaries (73), and surface facets (65). Further combination with other in situ measurements will allow for reliable verification of this hypothesis in this complex environment.

REACTION INTERMEDIATES

Electrochemical Mass Spectrometry

Electrochemical mass spectrometry (EMS) is an analytical technique that integrates an electrochemical analysis with MS. A typical EMS consists of an electrochemical cell, a microporous hydrophobic membrane (e.g., polytetrafluoroethylene), and a vacuum system with MS. The hydrophobic membrane's role is to prevent electrolyte penetration into the vacuum chamber. The membrane porosity allows analysis of only the volatile and/or gas products (**Figure 6*a***). Membrane properties are essential for EMS applications. A typical membrane has a thickness of 60–75 μm, a nominal pore size in the range of 20–200 nm, and a porosity of 50%. During the last decades, different EMS variants have been developed based on various characteristics, such as the analytical system, collection method, electrochemical cell, or ionization method (8, 74–77). All these techniques allow the in situ/operando detection of gaseous and/or volatile reactants, intermediates, and products, obtaining a fast (0.1–10-s) qualitative and quantitative impression at the electrode surface during an electrochemical reaction. In a typical EMS experiment, the mass-to-charge ratios of different species produced in an electrochemical reaction are measured selectively as a function of applied potential, current, or time. Therefore, the correlation of ion currents corresponding to given species with an electrochemical technique enables mechanistic understanding of the electrochemical reaction. EMS methods can (*a*) detect reactive gas and/or volatile intermediates and products with excellent sensitivity, (*b*) obtain mass signals in a short time, and (*c*) measure the product reaction rate (in some applications).

EMS cells vary in their applications. Single-thin-layer experimental setups were developed to study single-crystal electrodes (**Figure 6*b***). The products or intermediates produced at the electrode surface diffuse through a thin electrolyte layer of 50–100 μm to reach the vacuum chamber within 2 s. In this configuration, the diffusion of electrochemical species competes with the electrolyte flux, leading a considerable part of the product to exit the cell before it can reach the Teflon membrane.

In the conventional cell, the electrocatalyst is deposited directly onto the hydrophobic membrane (**Figure 6*c***). Because the distance of the catalyst surface from the vacuum chamber is

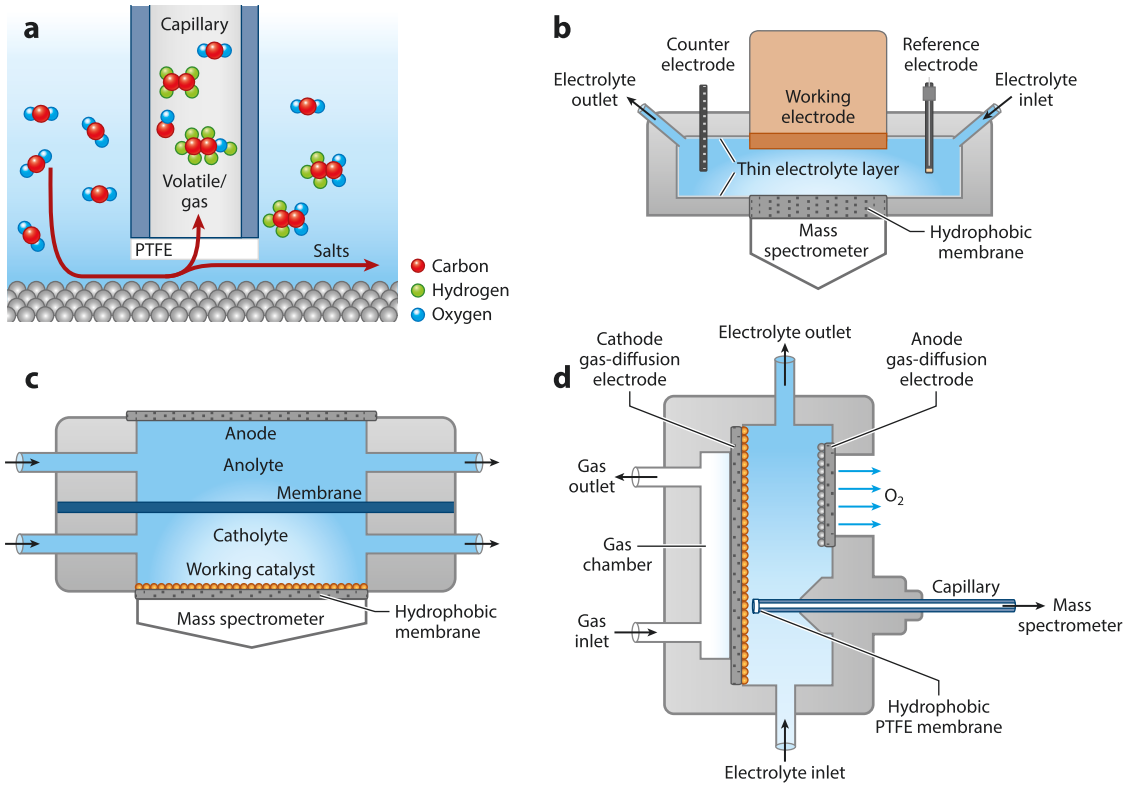

Figure 6

Cell design for electrochemical mass spectrometry. (*a*) Working principle of an electrochemical mass spectrometry configuration. (*b*) Single-thin-layer flow differential electrochemical mass spectrometry cell. (*c*) Dual-thin-layer differential electrochemical mass spectrometry. (*d*) Flow electrolyzer mass spectrometry configuration. Abbreviation: PTFE, polytetrafluoroethylene.

minimized, these reactors show the fastest detection time of approximately 0.1 s. The reactant diffusion into the active catalyst sites and the mechanical stability of the electrode are the main challenges of this setup.

Both single-thin-layer and conventional cells use batch or semi-batch reactors, inducing mass transport limitations to the system. A flow electrolyzer operating at high current densities (>100 mA cm^{-2}) can be used to overcome mass transport issues. The flow electrolyzer can provide insightful information about highly reactive intermediates at high reaction rates by incorporating a capillary (several micrometers in diameter) covered by a hydrophobic membrane (**Figure 6*d***). The planar diffusion of the species away from the capillary surface leads to a complicated time dependence and more significant response times.

Operando MS has been used as an analytical technique for the online detection of volatile and gaseous intermediates/products during electrochemical CO_2 reduction (8, 9, 19, 74, 76). Arán-Ais et al. (78) applied differential electrochemical mass spectrometry (DEMS) to study the effect of in situ surface modification on product selectivity. The authors investigated the impact of pulsed potential on Cu_2O transformation. Alcohol selectivity (mass-to-charge ratio of 31) showed a twofold increase under pulsed conditions. Simultaneously, the low mass signal intensity and the shift to more negative potentials of hydrogen ($m/z = 2$), methane ($m/z = 15$), and ethylene ($m/z = 26$) confirm their suppression under pulsed conditions. Combining DEMS with AFM, they concluded that the coexistence of Cu(I) and Cu tunes ethanol/n-propanol selectivity (**Figure 7*a***).

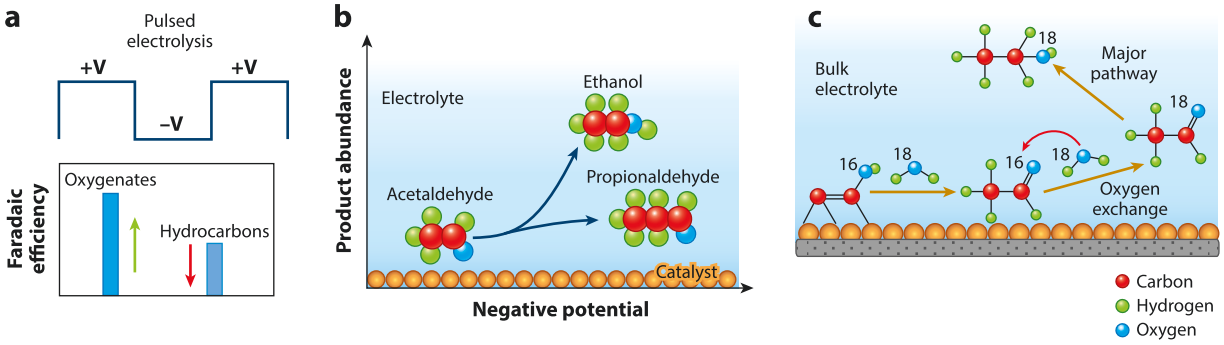

Figure 7

Electrochemical mass spectrometry experiments. (*a*) Pulsed electrolysis favors the formation of oxygenates at the expense of hydrocarbons. (*b*) High aldehyde abundance at the proximity of the electrode surface. Ethanol and propionaldehyde compete for the same intermediate. (*c*) Oxygen exchange between water and acetaldehyde occurs at the electrode surface.

Another study showed the importance of monitoring the local reaction environment using a DEMS setup with the catalyst layer deposited on a hydrophobic polytetrafluoroethylene membrane (79) (**Figure 7*b***). Results from this work indicate that aldehyde concentration (acetaldehyde and propionaldehyde) is significantly higher at the electrode vicinity compared to the corresponding alcohols (ethanol and n-propanol). Ethanol and propionaldehyde production rates have an opposite trend at more negative potentials, suggesting that they may compete for the same intermediate, such as acetaldehyde. The further reduction of propionaldehyde at the electrode vicinity leads to n-propanol production.

Hasa et al. (77) developed an alternative version of EMS, which uses a flow electrolyzer and a catalyst coated in a gas-diffusion layer. Through this method and isotopic labeling experiments, the authors investigated the origin of oxygen in the as-produced acetaldehyde (**Figure 7*c***). The results showed clear evidence that most of the produced acetaldehyde contains reactant oxygen, which undergoes fast oxygen exchange with the aqueous electrolyte. In addition, co-feeding of a postulated intermediate, such as acetaldehyde, demonstrated that the ethanol production rate increased while the signal of C_3 products remained constant. The latter indicates that the cross-coupling between CO and acetaldehyde is not the main pathway toward C_3 product formation. These two experiments demonstrate the advantages of this technique by detecting reactive species, incorporating isotopic labeling experiments, and co-feeding postulated intermediates to gain a mechanistic understanding of the reaction mechanism.

EMS in the CO_2 electroreduction reaction is normally used for qualitative analysis. The partial water pressure influences signal sensitivity, making the product quantification very challenging. In addition, nonvolatile products, such as acetate, cannot be detected with EMS. Using flow electrolyzer MS provides the opportunity to collect intermediates at high concentrations; however, the collection time is significantly higher than in batch cell configurations.

PERSPECTIVE

In situ and operando techniques have gained significant attention in optimizing CO_2RR analysis and enabling a better understanding of reaction conditions. Their use has advanced the CO_2RR field, in which different reaction pathways and stabler and more active catalysts have been suggested and designed. We show the progress of in situ/operando techniques during CO_2RR through some recent studies. These studies provide a representative picture of the information one can gain from each technique.

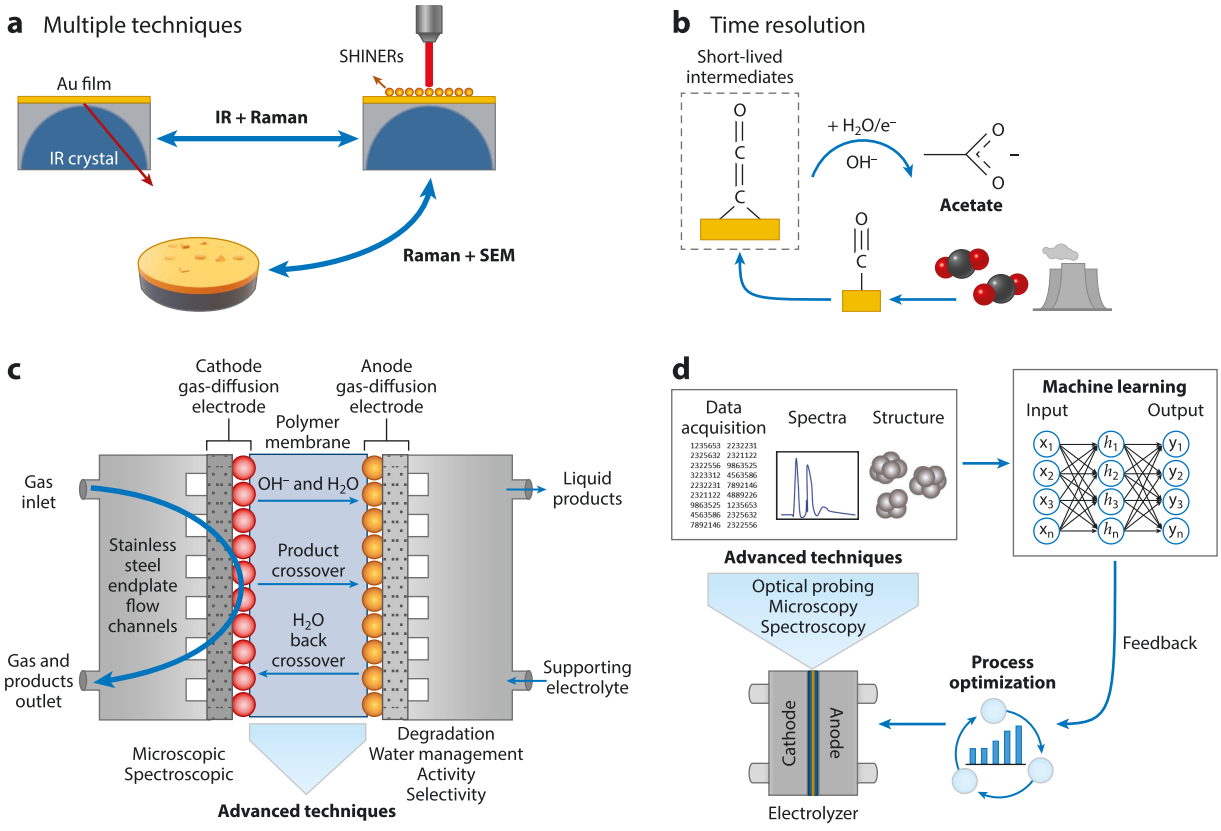

Figure 8

Schematic representation of the perspectives. (*a*) Combination of multiple techniques. (*b*) Faster data acquisition. (*c*) Advanced techniques for high–reaction rate cells. (*d*) Combination of computational and experimental analysis. Abbreviations: IR, infrared; SEM, scanning electron microscopy; SHINER, shell-isolated nanoparticle-enhanced Raman spectroscopy.

Despite the impressive achievements in developing in situ/operando tools, multiple factors hinder our understanding of complex electrochemical reactions. We suggest the following to gain a coherent picture of the relation of catalyst/electrode morphology with its activity, selectivity, and stability:

1. Most species detected by the spectroscopic methods are the species anchoring strongly on the surface, which may be poisoning to the electrocatalysis. For example, the observed surface oxide species on SERS proved to be unrelated to CORR performance; some other active intermediates, which cannot be detected on SERS due to their small amounts, may dominate in producing the products (15). In most cases, adsorbed CO is the only detectable intermediate in CO_2RR/CORR, providing minimal information on active sites. Given the inherent limitations of each method, the integrated use of various in situ/operando techniques is essential to reveal a comprehensive picture of the process under dynamic conditions (**Figure 8*a***). These methods would provide a route for the simultaneous analysis of adsorbates, intermediates, and morphological/chemical changes of the catalyst. For example, the combined use of microscopic (e.g., STEM, AFM) and spectroscopic (e.g., RAMAN, XAS, MS) methods may reveal specific information on how the coordination

environment, chemical state, and evolution of products/intermediates are correlated. More studies should employ inductively coupled plasma mass spectrometry (ICP-MS) to fully understand the catalyst degradation mechanism and associate it with its activity and selectivity. This technique detects dissolved metal ions and investigates how reaction conditions lead to metal particle dissolution or detachment. Integrating ICP-MS with additional operando methods is crucial to provide a framework that correlates catalyst degradation mechanisms, structure/chemical states, and reaction intermediates/products during CO_2RR.

2. To date, most of the widely used in situ/operando techniques detect reaction intermediates or adsorbed species in the time frame of seconds or minutes. The impact of short-lifetime intermediates on catalyst changes (chemical state, structure, and degradation) has not been adequately validated experimentally due to the time-resolved limitations of each available technique. For example, theoretical studies predict the existence of ketene ($^*C=C=O$) as an intermediate during CO_2RR (80, 81). The presence of surface ketene at high pH explains acetate formation through direct OH^- attack of a ketene intermediate (82). However, experimental evidence of such reactive species with a very short lifetime is still lacking. Recent Raman spectrum achieves a 0.7-s time resolution to collect the CO signals (83). Still, developing and using time-resolved techniques on a time scale of milliseconds or picoseconds is highly desirable to improve interpretation of the collected data (**Figure 8*b***).
3. For practical applications, CO_2RR should be performed in a continuous flow cell to circumvent mass flow limitations and achieve high reaction rates. The accumulation of the reaction intermediates would be beneficial for validating the results on surface-enhanced vibrational spectroscopies. However, gas-fed devices are much more complex, involving nanostructured catalysts, ionomers, and porous gas-diffusion layers. This is a significant reason why the results obtained from a batch cell may not represent CO_2RR at high reaction rates. In situ/operando techniques capable of industrially relevant reaction conditions would benefit the community (**Figure 8*c***). In this regard, the dynamic catalyst changes induced by electrode wettability are less explored. Future efforts must be directed toward understanding the substrate's role in electrolysis performance. For example, how does interface wettability impact catalyst particle dissolution, chemical state, or reconstruction? Which are the catalyst degradation mechanisms under the different wetting states? More insights into the degradation mechanism could be gained by integrating emerging microscopy (STEM, AFM) with other advanced in situ/operando techniques, such as ICP-MS and in situ fluorescence electrochemical spectroscopy (84, 85). Last, in situ/operando techniques must be developed for membrane electrode assembly (MEA) configurations. Challenges associated with MEA characterization derive from catalyst surface accessibility and the existence of an ion-conducting membrane, which may also affect catalyst properties. Fuel cell studies can inspire the CO_2RR community to design cells capable of conducting in situ/operando studies (86). One example is X-ray computed tomography, which investigates the behavior of an MEA instead of the catalyst itself.
4. Finally, experimental data must be combined with theoretical studies (**Figure 8*d***). The complexity of electrochemical reactions requires using and developing computational software and methods to interpret experimental operando data. Theoretical studies are shifting from 0 K and ultrahigh-vacuum models to computational operando investigations (87). Consequently, combining operando experimental and computational analysis will significantly increase our ability to gain deeper insights into the relationship between reaction mechanisms and catalyst morphology/activity/selectivity/stability. Implementation of multiple in situ/operando (theoretical and experimental) methods will increase the amount of collected data. We expect that accurately determining the collected data will require multivariate

analysis approaches, such as machine learning. Machine learning is an exciting methodology to elucidate experimental data correlations, develop spectroscopy analysis models, and combine them with theoretical data (DFT) (88–91). As for experiment-driven machine learning, stimulation of catalyst properties allows testing of new designs without the need for physical experiments. This will enable the deterministic synthesis of catalysts with superior properties for CO_2RR. Also, machine learning models trained by DFT simulations can avoid time-consuming and costly experiments and/or quantum-chemical calculations.

Overall, emerging in situ/operando technologies could open exciting research avenues for identifying active sites and uncovering mechanistic pathways that will lead to design of highly active/selective CO_2RR catalysts for practical applications.

DISCLOSURE STATEMENT

The authors are not aware of any affiliations, memberships, funding, or financial holdings that might be perceived as affecting the objectivity of this review.

ACKNOWLEDGMENTS

The authors would like to thank financial support from the National Science Foundation (CBET-1904966).

LITERATURE CITED

1. Hepburn C, Adlen E, Beddington J, Carter EA, Fuss S, Mac Dowell N, et al. 2019. The technological and economic prospects for CO_2 utilization and removal. *Nature* 575:87–97
2. Jouny M, Luc W, Jiao F. 2018. High-rate electroreduction of carbon monoxide to multi-carbon products. *Nat. Catal.* 1:748–55
3. Luc W, Fu X, Shi J, Lv J-J, Jouny M, et al. 2019. Two-dimensional copper nanosheets for electrochemical reduction of carbon monoxide to acetate. *Nat. Catal.* 2:423–30
4. De Luna P, Hahn C, Higgins D, Jaffer SA, Jaramillo TF, Sargent EH. 2019. What would it take for renewably powered electrosynthesis to displace petrochemical processes? *Science* 364:350
5. Gabardo CM, O'Brien CP, Edwards JP, McCallum C, Xu Y, et al. 2019. Continuous carbon dioxide electroreduction to concentrated multi-carbon products using a membrane electrode assembly. *Joule* 3:2777–91
6. Handoko AD, Wei F, Jenndy Yeo BS, Seh ZW. 2018. Understanding heterogeneous electrocatalytic carbon dioxide reduction through operando techniques. *Nat. Catal.* 1:922–34
7. Zhu Y, Wang J, Chu H, Chu Y-C, Chen HM. 2020. In situ/operando studies for designing next-generation electrocatalysts. *ACS Energy Lett.* 5:1281–91
8. Khanipour P, Loffler M, Reichert AM, Haase FT, Mayrhofer KJJ, Katsounaros I. 2019. Electrochemical real-time mass spectrometry (EC-RTMS): monitoring electrochemical reaction products in real time. *Angew. Chem. Int. Ed.* 58:7273–77
9. Löffler M, Khanipour P, Kulyk N, Mayrhofer KJJ, Katsounaros I. 2020. Insights into liquid product formation during carbon dioxide reduction on copper and oxide-derived copper from quantitative real-time measurements. *ACS Catal.* 10:6735–40
10. Dutta A, Rahaman M, Hecker B, Drnec J, Kiran K, et al. 2020. CO_2 electrolysis—complementary *operando* XRD, XAS and Raman spectroscopy study on the stability of Cu_xO foam catalysts. *J. Catal.* 389:592–603
11. Schlüter N, Novák P, Schröder D. 2022. Nonlinear electrochemical analysis: worth the effort to reveal new insights into energy materials. *Adv. Energy Mater.* 12:2200708.
12. Mendoza D, Dong S-T, Lassalle-Kaiser B. 2022. *In situ/operando* X-ray spectroscopy applied to electrocatalytic CO_2 reduction: status and perspectives. *Curr. Opin. Colloid Interface Sci.* 61:101635
13. Li X, Wang S, Li L, Sun Y, Xie Y. 2020. Progress and perspective for in situ studies of CO_2 reduction. *J. Am. Chem. Soc.* 142:9567–81

14. Cao X, Tan D, Wulan B, Hui KS, Hui KN, et al. 2021. In situ characterization for boosting electrocatalytic carbon dioxide reduction. *Small Methods* 5:2100700
15. Zhao Y, Chang X, Malkani AS, Yang X, Thompson L, et al. 2020. Speciation of Cu surfaces during the electrochemical CO reduction reaction. *J. Am. Chem. Soc.* 142:9735–43
16. Chang X, Zhao Y, Xu B. 2020. pH dependence of Cu surface speciation in the electrochemical CO reduction reaction. *ACS Catal.* 10:13737–47
17. Malkani AS, Li J, Oliveira NJ, He M, Chang X, et al. 2020. Understanding the electric and nonelectric field components of the cation effect on the electrochemical CO reduction reaction. *Sci. Adv.* 6:eabd2569
18. Malkani AS, Anibal J, Chang X, Xu B. 2020. Bridging the gap in the mechanistic understanding of electrocatalysis via in situ characterizations. *iScience* 23:101776
19. Wang X, de Araujo JF, Ju W, Bagger A, Schmies H, et al. 2019. Mechanistic reaction pathways of enhanced ethylene yields during electroreduction of CO_2-CO co-feeds on Cu and Cu-tandem electrocatalysts. *Nat. Nanotechnol.* 14:1063–70
20. Moller T, Scholten F, Thanh TN, Sinev I, Timoshenko J, et al. 2020. Electrocatalytic CO_2 reduction on CuO_x nanocubes: tracking the evolution of chemical state, geometric structure, and catalytic selectivity using operando spectroscopy. *Angew. Chem. Int. Ed.* 59:17974–83
21. Lin SC, Chang CC, Chiu SY, Pai HT, Liao TY, et al. 2020. Operando time-resolved X-ray absorption spectroscopy reveals the chemical nature enabling highly selective CO_2 reduction. *Nat. Commun.* 11:3525
22. Farmand M, Landers AT, Lin JC, Feaster JT, Beeman JW, et al. 2019. Electrochemical flow cell enabling *operando* probing of electrocatalyst surfaces by X-ray spectroscopy and diffraction. *Phys. Chem. Chem. Phys.* 21:5402–8
23. Arán-Ais RM, Rizo R, Grosse P, Algara-Siller G, Dembele K, et al. 2020. Imaging electrochemically synthesized Cu_2O cubes and their morphological evolution under conditions relevant to CO_2 electroreduction. *Nat. Commun.* 11:3489
24. Simon GH, Kley CS, Roldan Cuenya B. 2020. Potential-dependent morphology of copper catalysts during CO_2 electroreduction revealed by in situ atomic force microscopy. *Angew. Chem. Int. Ed.* 60:2561–68
25. Grosse P, Gao D, Scholten F, Sinev I, Mistry H, Roldan Cuenya B. 2018. Dynamic changes in the structure, chemical state and catalytic selectivity of Cu nanocubes during CO_2 electroreduction: size and support effects. *Angew. Chem. Int. Ed.* 57:6192–97
26. Jiang K, Huang Y, Zeng G, Toma FM, Goddard WA, Bell AT. 2020. Effects of surface roughness on the electrochemical reduction of CO_2 over Cu. *ACS Energy Lett.* 5:1206–14
27. Bergmann A, Roldan Cuenya B. 2019. Operando insights into nanoparticle transformations during catalysis. *ACS Catal.* 9:10020–43
28. Zhang Y, Guo S-X, Zhang X, Bond AM, Zhang J. 2020. Mechanistic understanding of the electrocatalytic CO_2 reduction reaction—new developments based on advanced instrumental techniques. *Nano Today* 31:100835
29. Dwyer JR, Harb M. 2017. Through a window, brightly: a review of selected nanofabricated thin-film platforms for spectroscopy, imaging, and detection. *Appl. Spectrosc.* 71:2051–75
30. Vavra J, Shen TH, Stoian D, Tileli V, Buonsanti R. 2021. Real-time monitoring reveals dissolution/redeposition mechanism in copper nanocatalysts during the initial stages of the CO_2 reduction reaction. *Angew. Chem. Int. Ed.* 60:1347–54
31. Kaliva M, Vamvakaki M. 2020. Chapter 17: nanomaterials characterization. In *Polymer Science and Nanotechnology*, ed. R Narain, pp. 401–33. Amsterdam: Elsevier
32. Scott SB, Hogg TV, Landers AT, Maagaard T, Bertheussen E, et al. 2019. Absence of oxidized phases in Cu under CO reduction conditions. *ACS Energy Lett.* 4:803–4
33. Ahn S, Klyukin K, Wakeham RJ, Rudd JA, Lewis AR, et al. 2018. Poly-amide modified copper foam electrodes for enhanced electrochemical reduction of carbon dioxide. *ACS Catal.* 8:4132–42
34. Zhai Y, Han P, Yun Q, Ge Y, Zhang X, et al. 2022. Phase engineering of metal nanocatalysts for electrochemical CO_2 reduction. *eScience* 2:467–85
35. Sheng W, Kattel S, Yao S, Yan B, Liang Z, et al. 2017. Electrochemical reduction of CO_2 to synthesis gas with controlled CO/H_2 ratios. *Energy Environ. Sci.* 10:1180–85

36. Timoshenko J, Roldan Cuenya B. 2021. *In situ/operando* electrocatalyst characterization by X-ray absorption spectroscopy. *Chem. Rev.* 121:882–961
37. Jeon HS, Timoshenko J, Scholten F, Sinev I, Herzog A, et al. 2019. Operando insight into the correlation between the structure and composition of CuZn nanoparticles and their selectivity for the electrochemical CO_2 reduction. *J. Am. Chem. Soc.* 141:19879–87
38. Ebaid M, Jiang K, Zhang Z, Drisdell WS, Bell AT, Cooper JK. 2020. Production of C_2/C_3 oxygenates from planar copper nitride-derived mesoporous copper via electrochemical reduction of CO_2. *Chem. Mater.* 32:3304–11
39. Gao D, Arán-Ais RM, Jeon HS, Roldan Cuenya B. 2019. Rational catalyst and electrolyte design for CO_2 electroreduction towards multicarbon products. *Nat. Catal.* 2:198–210
40. Li F, Li YC, Wang Z, Li J, Nam D-H, et al. 2019. Cooperative CO_2-to-ethanol conversion via enriched intermediates at molecule–metal catalyst interfaces. *Nat. Catal.* 3:75–82
41. Chou TC, Chang CC, Yu HL, Yu WY, Dong CL, et al. 2020. Controlling the oxidation state of the Cu electrode and reaction intermediates for electrochemical CO_2 reduction to ethylene. *J. Am. Chem. Soc.* 142:2857–67
42. Ko BH, Hasa B, Shin H, Jeng E, Overa S, et al. 2020. The impact of nitrogen oxides on electrochemical carbon dioxide reduction. *Nat. Commun.* 11:5856
43. Verdaguer-Casadevall A, Li CW, Johansson TP, Scott SB, McKeown JT, et al. 2015. Probing the active surface sites for CO reduction on oxide-derived copper electrocatalysts. *J. Am. Chem. Soc.* 137:9808–11
44. Lee SH, Sullivan I, Larson DM, Liu G, Toma FM, et al. 2020. Correlating oxidation state and surface area to activity from operando studies of copper CO electroreduction catalysts in a gas-fed device. *ACS Catal.* 10:8000–11
45. Zhao Y, Du L, Li H, Xie W, Chen J. 2019. Is the Suzuki-Miyaura cross-coupling reaction in the presence of Pd nanoparticles heterogeneously or homogeneously catalyzed? An interfacial surface-enhanced Raman spectroscopy study. *J. Phys. Chem. Lett.* 10:1286–91
46. Zhao Y, Zhang X-G, Bodappa N, Yang W-M, Liang Q, et al. 2022. Elucidating electrochemical CO_2 reduction reaction processes on Cu(*hkl*) single-crystal surfaces by *in situ* Raman spectroscopy. *Energy Environ. Sci.* 15:3968–77
47. Ren D, Ang BS-H, Yeo BS. 2016. Tuning the selectivity of carbon dioxide electroreduction toward ethanol on oxide-derived Cu_xZn catalysts. *ACS Catal.* 6:8239–47
48. Dutta A, Kuzume A, Rahaman M, Vesztergom S, Broekmann P. 2015. Monitoring the chemical state of catalysts for CO_2 electroreduction: an in operando study. *ACS Catal.* 5:7498–502
49. Yang H, Hu Y-W, Chen J-J, Balogun MS, Fang P-P, et al. 2019. Intermediates adsorption engineering of CO_2 electroreduction reaction in highly selective heterostructure Cu-based electrocatalysts for CO production. *Adv. Energy Mater.* 9:1901396
50. He M, Li C, Zhang H, Chang X, Chen JG, et al. 2020. Oxygen induced promotion of electrochemical reduction of CO_2 via co-electrolysis. *Nat. Commun.* 11:3844
51. Li F, Thevenon A, Rosas-Hernández A, Wang Z, Li Y, et al. 2020. Molecular tuning of CO_2-to-ethylene conversion. *Nature* 577:509–13
52. Weitzner SE, Akhade SA, Varley JB, Wood BC, Otani M, et al. 2020. Toward engineering of solution microenvironments for the CO_2 reduction reaction: unraveling pH and voltage effects from a combined density-functional–continuum theory. *J. Phys. Chem. Lett.* 11:4113–18
53. Gao J, Zhang H, Guo X, Luo J, Zakeeruddin SM, et al. 2019. Selective C–C coupling in carbon dioxide electroreduction via efficient spillover of intermediates as supported by operando Raman spectroscopy. *J. Am. Chem. Soc.* 141:18704–14
54. Chen X, Henckel DA, Nwabara UO, Li Y, Frenkel AI, et al. 2020. Controlling speciation during CO_2 reduction on Cu-alloy electrodes. *ACS Catal.* 10:672–82
55. Zeng Z-C, Hu S, Huang S-C, Zhang Y-J, Zhao W-X, et al. 2016. Novel electrochemical Raman spectroscopy enabled by water immersion objective. *Anal. Chem.* 88:9381–85
56. Luo M, Wang Z, Li YC, Li J, Li F, et al. 2019. Hydroxide promotes carbon dioxide electroreduction to ethanol on copper via tuning of adsorbed hydrogen. *Nat. Commun.* 10:5814
57. Lu X, Zhu C, Wu Z, Xuan J, Francisco JS, Wang H. 2020. In situ observation of the pH gradient near the gas diffusion electrode of CO_2 reduction in alkaline electrolyte. *J. Am. Chem. Soc.* 142:15438–44

58. Henckel DA, Counihan MJ, Holmes HE, Chen X, Nwabara UO, et al. 2020. Potential dependence of the local pH in a CO_2 reduction electrolyzer. *ACS Catal.* 11:255–63
59. Lv J-J, Jouny M, Luc W, Zhu W, Zhu J-J, Jiao F. 2018. A highly porous copper electrocatalyst for carbon dioxide reduction. *Adv. Mater.* 30:1803111
60. Yang KL, Kas R, Smith WA. 2019. In situ infrared spectroscopy reveals persistent alkalinity near electrode surfaces during CO_2 electroreduction. *J. Am. Chem. Soc.* 141:15891–900
61. Wright D, Lin Q, Berta D, Földes T, Wagner A, et al. 2021. Mechanistic study of an immobilized molecular electrocatalyst by in situ gap-plasmon-assisted spectro-electrochemistry. *Nat. Catal.* 4:157–63
62. Malkani AS, Li J, Anibal J, Lu Q, Xu B. 2020. Impact of forced convection on spectroscopic observations of the electrochemical CO reduction reaction. *ACS Catal.* 10:941–46
63. Gunathunge CM, Li X, Li J, Hicks RP, Ovalle VJ, Waegele MM. 2017. Spectroscopic observation of reversible surface reconstruction of copper electrodes under CO_2 reduction. *J. Phys. Chem. C* 121:12337–44
64. Gunathunge CM, Li JY, Li X, Hong JLJ, Waegele MM. 2020. Revealing the predominant surface facets of rough Cu electrodes under electrochemical conditions. *ACS Catal.* 10:6908–23
65. Malkani AS, Dunwell M, Xu B. 2019. Operando spectroscopic investigations of copper and oxide-derived copper catalysts for electrochemical CO reduction. *ACS Catal.* 9:474–78
66. Corson ER, Kas R, Kostecki R, Urban JJ, Smith WA, et al. 2020. In situ ATR-SEIRAS of carbon dioxide reduction at a plasmonic silver cathode. *J. Am. Chem. Soc.* 142:11750–62
67. Li JY, Li X, Gunathunge CM, Waegele MM. 2019. Hydrogen bonding steers the product selectivity of electrocatalytic CO reduction. *PNAS* 116:9220–29
68. Firet NJ, Smith WA. 2016. Probing the reaction mechanism of CO_2 electroreduction over Ag films via operando infrared spectroscopy. *ACS Catal.* 7:606–12
69. Kim Y, Park S, Shin SJ, Choi W, Min BK, et al. 2020. Time-resolved observation of C-C coupling intermediates on Cu electrodes for selective electrochemical CO_2 reduction. *Energy Environ. Sci.* 13:4301–11
70. Pérez-Gallent E, Figueiredo MC, Calle-Vallejo F, Koper MTM. 2017. Spectroscopic observation of a hydrogenated CO dimer intermediate during CO reduction on Cu(100) electrodes. *Angew. Chem. Int. Ed.* 56:3621–24
71. Patra KK, Park S, Song H, Kim B, Kim W, Oh J. 2020. Operando spectroscopic investigation of a boron-doped CuO catalyst and its role in selective electrochemical C–C coupling. *ACS Appl. Energy Mater.* 3:11343–49
72. Iijima G, Inomata T, Yamaguchi H, Ito M, Masuda H. 2019. Role of a hydroxide layer on Cu electrodes in electrochemical CO_2 reduction. *ACS Catal.* 9:6305–19
73. Chen Z, Wang T, Liu B, Cheng D, Hu C, et al. 2020. Grain-boundary-rich copper for efficient solar-driven electrochemical CO_2 reduction to ethylene and ethanol. *J. Am. Chem. Soc.* 142:6878–83
74. Schouten KJ, Qin Z, Perez Gallent E, Koper MT. 2012. Two pathways for the formation of ethylene in CO reduction on single-crystal copper electrodes. *J. Am. Chem. Soc.* 134:9864–67
75. Grote J-P, Zeradjanin AR, Cherevko S, Savan A, Breitbach B, et al. 2016. Screening of material libraries for electrochemical CO_2 reduction catalysts—improving selectivity of Cu by mixing with Co. *J. Catal.* 343:248–56
76. Mandal L, Yang KR, Motapothula MR, Ren D, Lobaccaro P, et al. 2018. Investigating the role of copper oxide in electrochemical CO_2 reduction in real time. *ACS Appl. Mater. Interfaces* 10:8574–84
77. Hasa B, Jouny M, Ko BH, Xu B, Jiao F. 2020. Flow electrolyzer mass spectrometry with a gas-diffusion electrode design. *Angew. Chem. Int. Ed.* 60:3277–82
78. Arán-Ais RM, Scholten F, Kunze S, Rizo R, Roldan Cuenya B. 2020. The role of in situ generated morphological motifs and Cu(I) species in C_{2+} product selectivity during CO_2 pulsed electroreduction. *Nat. Energy* 5:317–25
79. Clark EL, Bell AT. 2018. Direct observation of the local reaction environment during the electrochemical reduction of CO_2. *J. Am. Chem. Soc.* 140:7012–20
80. Cheng T, Fortunelli A, Goddard WA 3rd. 2019. Reaction intermediates during operando electrocatalysis identified from full solvent quantum mechanics molecular dynamics. *PNAS* 116:7718–22

81. Calle-Vallejo F, Koper MT. 2013. Theoretical considerations on the electroreduction of CO to C_2 species on Cu(100) electrodes. *Angew. Chem. Int. Ed.* 52:7282–85
82. Jouny M, Hutchings GS, Jiao F. 2019. Carbon monoxide electroreduction as an emerging platform for carbon utilization. *Nat. Catal.* 2:1062–70
83. An H, Wu L, Mandemaker LDB, Yang S, Ruiter J, et al. 2021. Sub-second time-resolved surface-enhanced Raman spectroscopy reveals dynamic CO intermediates during electrochemical CO_2 reduction on copper. *Angew. Chem. Int. Ed.* 60:16576–84
84. Shi R, Guo J, Zhang X, Waterhouse GIN, Han Z, et al. 2020. Efficient wettability-controlled electroreduction of CO_2 to CO at Au/C interfaces. *Nat. Commun.* 11:3028
85. Jovanovič P, Pavlišič A, Šelih VS, Šala M, Hodnik N, et al. 2014. New insight into platinum dissolution from nanoparticulate platinum-based electrocatalysts using highly sensitive in situ concentration measurements. *ChemCatChem* 6:449–53
86. Meyer Q, Zeng Y, Zhao C. 2019. In situ and operando characterization of proton exchange membrane fuel cells. *Adv. Mater.* 31:e1901900
87. Grajciar L, Heard CJ, Bondarenko AA, Polynski MV, Meeprasert J, et al. 2018. Towards *operando* computational modeling in heterogeneous catalysis. *Chem. Soc. Rev.* 47:8307–48
88. Ebikade EO, Wang Y, Samulewicz N, Hasa B, Vlachos D. 2020. Active learning-driven quantitative synthesis–structure–property relations for improving performance and revealing active sites of nitrogen-doped carbon for the hydrogen evolution reaction. *React. Chem. Eng.* 5:2134–47
89. Lansford JL, Vlachos DG. 2020. Infrared spectroscopy data- and physics-driven machine learning for characterizing surface microstructure of complex materials. *Nat. Commun.* 11:1513
90. Chen Y, Huang Y, Cheng T, Goddard WA. 2019. Identifying active sites for CO_2 reduction on dealloyed gold surfaces by combining machine learning with multiscale simulations. *J. Am. Chem. Soc.* 141:11651–57
91. Zhong M, Tran K, Min Y, Wang C, Wang Z, et al. 2020. Accelerated discovery of CO_2 electrocatalysts using active machine learning. *Nature* 581:178–83

Annual Review of Chemical and Biomolecular Engineering

Volume 14, 2023

Contents

Errata

An online log of corrections to *Annual Review of Chemical and Biomolecular Engineering* articles may be found at http://www.annualreviews.org/errata/chembioeng